Iranian Journal of Medical Physics
Vol. 9, No. 4, Autumn 2012, 283-292
Received: July 29, 2012; Accepted: December 25, 2012

Original Article

A New Method for Sperm Detection in Human Semen: Combination of Hypothesis Testing and Local Mapping of Wavelet Sub-Bands

Seyed Vahab Shojaedini[1*], Ali Kermani[2], Vahid Reza Nafisi[1]

Abstract

Introduction
Automated methods for sperm characterization in microscopic videos have some limitations such as: low contrast of the video frames and possibility of neighboring sperms to touch each other. In this paper a new method is introduced for detection of sperms in microscopic videos.
Materials and Methods
In this work, first microscopic videos are captured from specimens of human semen. Several frames of these videos are transformed to wavelet sub-bands and bit-related planes are constructed from wavelet sub-bands separately. Finally, the acquired bit planes are mapped by different local mapping functions and decision is made using continuity and discontinuity of the mapping results. Based on the above decision procedure, each region of the microscopic image is assigned to either a sperm or other parts of semen.
Results
Performance of the proposed method was evaluated by two sets of microscopic videos which have been captured from semen of some infertile men. The first sets belonged to semen specimens with low densities of sperms and the second set belonged to semen specimens with high densities of sperms.
Conclusion
The results of this study revealed that the proposed method in this work is more efficient in sperm detection and extraction compared with the current approaches in both scenarios. Furthermore, it is evident that for specimens with higher sperm densities the proposed method improved sperm detection also reduces false detection rate considerably.

Keywords: Detection, Hypothesis Testing, Mapping, Microscopic Video, Semen, Wavelet Sub-Bands

1- Electrical Engineering Department, Iranian Research Organization for Science and Technology, Tehran, Iran
*Corresponding author: Tel: +98 21 8822107; Email: shojadini@irost.org
2- Electrical Engineering Department, Iran University of Science and Technology

1. Introduction

Infertility is a medical condition faced by 15% of couples worldwide [1]. Reliable reports have determined that male impotence is the main factor in 30-40% of all the infertility cases [2]. Men fertility depends on several factors, but the sperms have the key role in this procedure. Therefore, estimating sperm parameters has been one of the most favorite policies of researchers in infertility monitoring and cure [3, 4].

In recent years, modern microscopic imaging has provided ability of analyzing of semen [5-8]. In this method, the potential of fertility in men is determined by computing the parameters of sperms existing in microscopic images of semen. Some of these parameters are size, morphology, and their motion trajectory [9]. Based on above separating sperms from other particles of semen is a vital step for analyzing fertility [10]. Several methods have been used for such a discrimination which the oldest one is manually sperm detection by an expert person. Unfortunately this method is time-consuming and its performance is degraded by human errors [11]. Therefore, the automated methods have been substituted for processing these images. The main challenges which limit the performance of the automated methods are: the low contrast of the video frames, changing number of active sperms in several frames, and finally the possibility of neighboring sperms to touch each other so they may be considered as merged sperms [12]. Several approaches have been proposed to solve problems of automatic sperm detection methods. Some approaches utilize pixel-based techniques for separating sperms from other semen particles. For instance in [13] sperms have been detected using a threshold which has been calculated directly from intensity of pixels of microscopic images. In some other improved techniques, the above threshold changes adaptively during several successive frames [14]. In some researches, several types of 2D wavelet transform have been utilized for distinguishing of sperms from other parts of the semen [15-17]. Although such pixel-based methods have improved speed in sperm detection but they often cause considerable errors in low SNR microscopic images because of their sensitivity to noise [18]. There is a class of methods that separates sperms by using connectivity of pixels. Different contour-based methods may be suitable examples for the above class. Despite such methods show great ability to extract curve-shape boundaries belonging to head of sperms, they often need complementary post-processing to extract tail of sperms [19]. In another class of methods, the discontinuity between sperms and other particles of semen (e.g., background of microscopic image) is used to discriminate them. Several methods which are based on edge, gradient, Hilbert transform, and watershed segmentation are examples of the methods of this class which mainly handle the problem of extracting false particles in semen [20, 21].

In this paper, a new method is introduced for separating sperms from other particles of semen in microscopic video which works based on hypothesis testing. In the proposed method, first the 2D wavelet transform is applied on the microscopic image. In the second step, bit-plane images are constructed using the acquired wavelet sub-bands. Then, bit-plane images are mapped to connectivity space which leads to four mapped images. Finally, dependence of each pixel to sperm or the background is determined for mapped images using its connectivity factors. The bit-plane image processing is different for several images which are resulted from wavelet sub-bands. Thus, it may be concluded that the decision function of hypothesis testing for each region of microscopic image is constructed based on local characteristics of those regions. Therefore, such a decision function leads to more accurate decision about the presence of sperms in each region.

In section 2, the proposed algorithm is described mathematically which includes acquisition obtaining wavelet sub-bands, bit-planes, mapping, and construction decision function for hypothesis testing. In section 3, the performance of the proposed method is

evaluated for two real scenarios, one with low density of sperms and the other one with high density of sperms. In section 4, the experimental results are compared with results of several existing methods using their actual parameters. Conclusion is presented in the last section of the manuscript.

2. Materials and Methods

Suppose I as a microscopic video captured from semen specimen and I_t is one of its frames which is appeared in time slot t. The image I_t includes sperms, plasma, and debris. In this article the two latter parameters are called artifact. Also, it contains some amount of noise. For each pixel of I_t it can be written:

$$I_{tmj} = I_t(m, j) \quad 1 \le m \le M \;,\; 1 \le j \le J \;,\; 1 \le t \le T \tag{1}$$

In equation (1), I_{tmj} is the intensity of a pixel in I_t which is located in row and column equal with m and j, respectively. Also, M and J are the image sizes and T is the time length of video I. A different image is formed by the two frames of I which appeared in time slots t and t_0 as:

$$D_{tmj} = I_{tmj} - I_{(t-t_0)mj} \tag{2}$$

In which D_{tmj} is the intensity of the pixel which is located in row and column equal with m and j of the different image D_t, respectively. Now, dependence of D_{tmj} to sperm or artifact is determined by using hypothesis testing which is introduced in equation (3).

$$\begin{cases} H_0: & D_{tmj} = \left| g_{tmj} + n_{tmj} \right| \\ H_1: & D_{tmj} = \left| s_{tmj} + g_{tmj} + n_{tmj} \right| \end{cases} \tag{3}$$

In this equation H_0 shows the dependence of D_{tmj} to artifact and noise while H_1 shows its dependence to sperm. Also s_{tmj}, g_{tmj} and n_{tmj} show sperm, artifact and noise components in D_{tmj}. Computing the second level discrete wavelet transform [22] of D_t four sub-bands is obtained which are called C_t^{λ} which their elements are C_{tmj}^{λ} that are located in row and column equal with m and j, respectively. These four sub-bands are mentioned as:

$$\lambda = \{LL, HL, LH, HH\} \tag{4}$$

The above set may be decomposed to sub-sets λ' and λ'' as:

$$\lambda'' = \{LL\} \quad , \quad \lambda' = \{HL, LH, HH\} \tag{5}$$

In the next step, each of the sub-bands C_t^{HL}, C_t^{LH} and C_t^{HH} are converted to K number of bit-planes such as $P_{tk}^{\lambda'}$ as:

$$P_{tmjk}^{\lambda'} = P_{tk}^{\lambda'}(m, j) \;,\; k = 1,2,...,K \tag{6}$$

In equation (6), the term $P_{tmjk}^{\lambda'}$ shows the bit which is located in position (m, j) of bit-plane k which is obtained from $C_t^{\lambda'}$. The maximum number of bit-planes is obtained from equation (7) [23]:

$$2^K = \max(\left| C_{tmj} \right|), \quad (m, j) \in \lambda \tag{7}$$

Now, the procedure which is mentioned bellow is applied to each bit of the bit-planes.

2.1. The feature set $C_t^{LL} = \{C_{tmj}^{LL}\}$ is extracted from a sliding window which is centered in (m, j) and its size is $(m_0 + 1) \times (j_0 + 1)$ as:

$$\{C_{tmj}^{LL}\} = \{C_{t(m-m_0)(j-j_0)}^{LL}, ..., C_{tmj}^{LL}, ..., C_{t(m+m_0)(j+j_0)}^{LL}\} \tag{8}$$

2.2. For $\{C_{tmj}^{LL}\}$ the mapping parameter U_{tmj}^{LL} is defined based on changes of the values of above sliding window as:

$$U_{tmj}^{LL}=\begin{cases}u & \text{If u different values exist in window}\\ 0 & \text{If there are no different values}\end{cases} \quad (9)$$

2.3. The mapping function is defined for all elements of C_t^{LL} based on mapping parameter U_{tmj}^{LL} as:

$$E_{tmj}^{LL}=C_{tmj}^{LL}+\alpha U_{tmj}^{LL}(C_{tmj}^{LL}-\overline{C_t^{LL}}) \quad (10)$$

In which E_{tmj}^{LL} shows mapped pixels of C_t^{LL} which make a mapped pseudo-image E_t^{LL}. Also, $\overline{C_t^{LL}}$ shows the mean of C_t^{LL}. Based on definition of U_{tmj}^{LL} (e.g., equation 9), the equation (10) shows that E_t^{LL} strongly depends on continuity and dis-continuity of C_t^{LL}. Now, E_t^{LL} is converted to K number of bit-planes P'^{LL}_{tk} in such way that equation (11) can be written similar to equation (6) as:

$$P'^{LL}_{tmjk}=P'^{LL}_{tk}(m,j):\ k=1,2,...,K \quad (11)$$

2.4. Consider P_{tmjk}^{LH} and its two horizontal neighbors. If at least two of these three bits are equal to "1" then $P'^{LH}_{tmjk}=1$ is substituted, otherwise $P'^{LH}_{tmjk}=0$ is replaced.

2.5. Consider P_{tmjk}^{HL} and its two vertical neighbors. If at least two of these three bits are equal to "1" then $P'^{HL}_{tmjk}=1$ is substituted, otherwise $P'^{HL}_{tmjk}=0$ is replaced.

2.6. Consider P_{tmjk}^{HH} and its four diagonal neighbors. If at least three of these five bits are equal to "1" then $P'^{HH}_{tmjk}=1$ is substituted, otherwise $P'^{HH}_{tmjk}=0$ is replaced.

By running above steps, the four bit-planes $P'^{LL}_t, P'^{LH}_t, P'^{HL}_t$, and P'^{HH}_t are obtained in accordance with four sub-bands of λ. Now, the processed image F_t is obtained by applying inverse 2D wavelet transform on P'_t which its wavelet sub-bands are $P'^{LL}_t, P'^{LH}_t, P'^{HL}_t$ and P'^{HH}_t. Finally, sperms in F_t are extracted as connected objects which are listed in equation (12), by using the labeling method which has been introduced in [24].

$$\{O_t\}=\{O_{t1},...,O_{tw},...,O_{tW}\} \quad (12)$$

In which $\{O_t\}$ is the set of detected sperms in time slot t, O_{tw} is the sperm w of this set and W is the total number of extracted sperms. Combining equations (3) and (13) dependence of each pixel of microscopic image is determined to sperm or artifact as:

$$\begin{cases}H_0: & F_{tmj}\notin O_t \ \Rightarrow\\ & D_{tmj}=|g_{tmj}+n_{tmj}|\\ H_1: & F_{tmj}\in O_t \ \Rightarrow\\ & D_{tmj}=|s_{tmj}+g_{tmj}+n_{tmj}|\end{cases} \quad (13)$$

Two standard parameters are defined to evaluate the performance of the proposed method. The first parameter is probability of detection and shows the ability of method in extracting correct sperms in presence of artifact and noise. It is defined as:

$$P_D=P(F_{tmj}\in O_t\,|\,H_1) \quad (14)$$

The second parameter is false detection error (false alarm) which shows the probability of detecting other semen particles as sperms. This parameter is defined as:

$$P_{fa}=P(F_{tmj}\in O_t\,|\,H_0) \quad (15)$$

3. Results

The proposed algorithm was applied to microscopic videos which were captured from human semen. The data collection setup contained a Nikon invert microscope using a 40x zoom lens and a Moticom480 digital CCD camera which was mounted on the microscope to record video. This setup is showed in figure

(1-a). A calibrated microscope slide was used for all experiments. This microscope slide is showed in figure (1-b) and it was scaled per 10 micrometer which enabled us to estimate size and movement parameters of sperms.

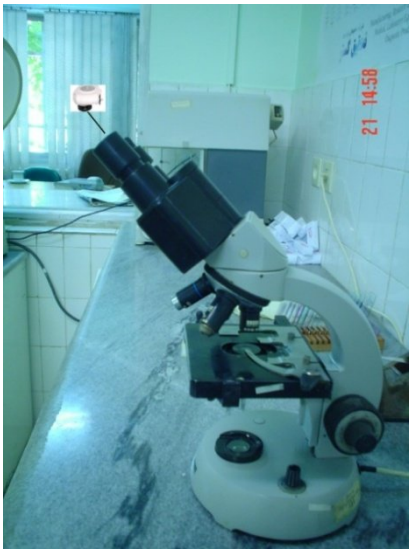

(a)

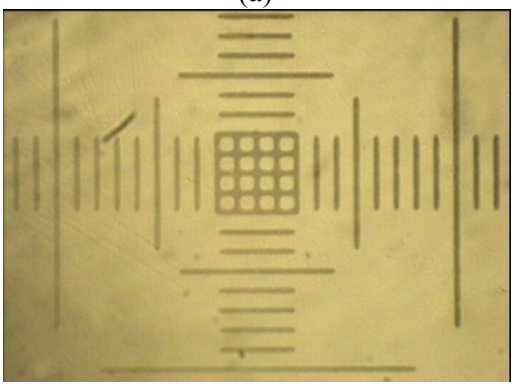

(b)

Figure 1. Data collection setup: (a) invert microscope, zoom lens and digital CCD, (b) calibrated and scaled microscope slide.

After calibration, the semen sample was put on a non-scaled microscope slide and digital videos were captured. The image of this non-scaled microscope slide existed in all captured frames as background. Therefore, the image of empty non-scaled microscope slide (which has been showed in figure (2) was subtracted from all captured frames for background elimination. Using this procedure, 135 frames of semen were investigated which belonged to 9 infertile men. The proposed method was implemented using Matlab 2009. Furthermore, Histogram Thresholding Segmentation algorithm (HTS) [25], Multi Structure Element Segmentation (MSES) [26], and Dynamic Threshold Segmentation (DTS) [14] were implemented to compare the results with the proposed algorithm. The captured videos firstly were processed manually to obtain a reference detection to compare with the four mentioned methods. Then, the performance of each algorithm was determined by computing its P_D and P_{fa} as described in equations (14) and (15).

Figure 2. Reference image from empty microscope slide

Tests were carried out on two different scenarios which in one of them, the semen specimens had low densities of sperms (bellow 2 million sperms per milliliter) so they were better distinguished in captured images. In the second scenario, specimens had high densities of sperms (more than 2 million sperms per milliliter), so their near distances led to degrading of detection. Specifications of both scenarios are been showed in table 1.

Table1. Specifications of test scenarios

Specification	Value	Specification	Value
Min and Max sizes of sperms	5 , 50 pixels	Number of captured frames	135
Frame size (pixels)	288*352	Min-Max velocity of sperms	1-3 pixels per frame
Number of samples	9 persons	Average contrast	15%
Frame rate	30 frames per second	Average noise change to sperm changes	0.75

Figure (3) shows results produced by the first scenario. Figure (3-a) shows the captured frame in which the sperms labeled manually while (3-b) and (3-c) show the results of processing this frame using the proposed method and HTS. It is obvious that the proposed method has extracted all 8 sperms which were labeled in figure (3-a) while HTS extracted only 5 sperms which one of them was extracted incompletely. Also, it can be seen that both methods have not extracted any false sperm.

Figure (4) shows one of the obtained results on captured images belonging to the second scenario. Figure (4-a) shows the captured frame in which the sperms labeled manually while (4-b) and (4-c) show the results of processing of this frame utilizing the proposed and HTS methods. It may be considered that the proposed method extracted 25 sperms (one of these sperms has been extracted incompletely) from total 32 manually labeled sperms while HTS extracted 12 sperms which four of them have been extracted incompletely. Also, it may be noted that although the proposed method extracted only one false sperm, the HTS detected 24 false sperms.

4. Discussion

Data which were obtained from microscopy of semen specimens with low and high densities of sperms were investigated. The proposed algorithm and three existing methods (MSES, DTS, and HTS) were implemented and the results were compared with manual detection. Probabilities for true and false detection were used as parameters for comparison. To compute probability of detection, two definitions for true detection were applied. In some infertility diagnostic applications, the only important parameter is the sperm population [27], while for other applications, the complete extraction of sperms is necessary because of the necessity to compute their length, morphology, and size. Based on these two definitions, probability of detection was computed in two different ways. In the first manner, the true extracted sperm was considered as a sperm with correct position in the image. In the second manner, the correct detection was considered as a sperm that at least 90% of its pixels were extracted correctly. Table 2 shows different performances for the proposed method and other sperm extraction techniques. Based on this table, in the first scenario, the results of the proposed method were 43%, 39%, and 37% better than DTS, MSES, and HTS by using probability of detection without size criteria as the comparison parameter. Theses superiorities reached 46%, 44%, and 40% when probability of detection with size criteria was used as the comparison parameter. Comparing false detection probabilities of these four methods shows that despite of considerable superiority in detection by the proposed algorithm, its false detection probability did not increase compared with other techniques.

Table 2 shows more considerable superiority for the proposed method in the second scenario. In this scenario, the results which have been obtained by using the proposed method were 43%, 41%, and 38% better than DTS, MSES, and HTS when the probability of detection without size criteria was used as the comparison parameter.

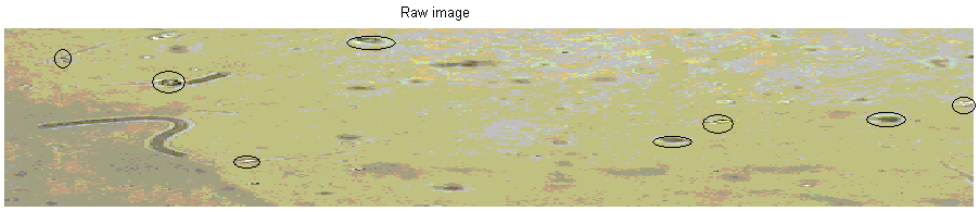

(a)

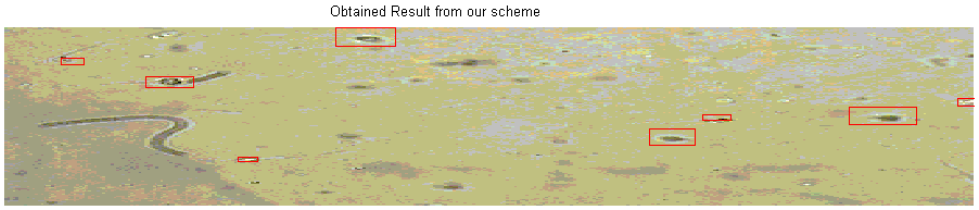

(b)

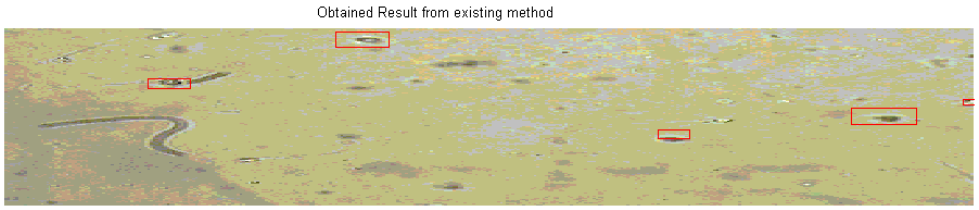

(c)

Figure 3. One of the results from the first scenario: (a) The captured microscopic images for a semen specimen in which the sperms have been labeled manually, (b) Extracted sperms using the proposed algorithm, and (c) Extracted sperms using HTS algorithm.

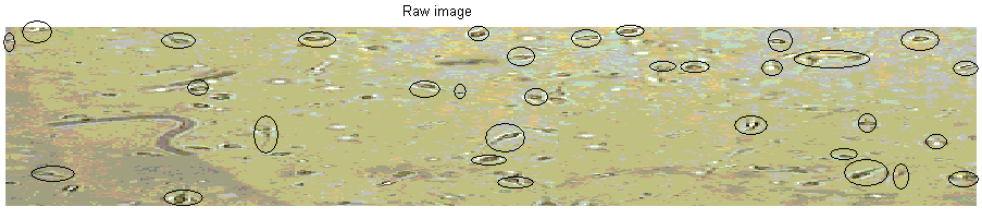

(a)

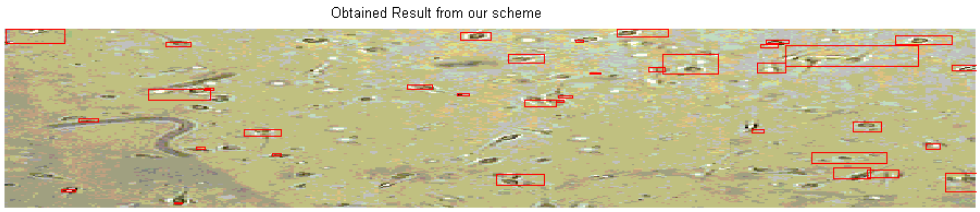

(b)

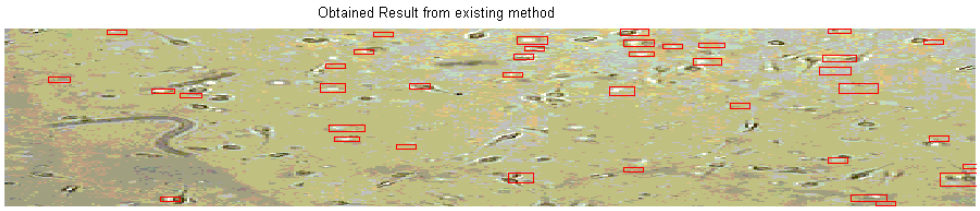

(c)

Figure 4. One of the results from the second scenario: (a) The captured microscopic images for a semen specimen in which the sperms have been labeled manually, (b) Extracted sperms using the proposed algorithm, and (c) Extracted sperms using HTS algorithm.

Table 2. Comparing the performances of the implemented algorithms in both of scenarios

Comparison Parameter	Images captured from semen with Low Density of Sperms (First Scenario)				Images captured from semen with High Density of Sperms (Second Scenario)			
	Proposed Method	DTS	MSES	HTS	Proposed Method	DTS	MSES	HTS
Probability of Detection (without size criteria)	87	44	48	50	77	34	36	39
Probability of Detection (with size criteria)	85	39	41	45	73	20	21	25
Probability of False Detection	4	5	4	3	5	51	47	48

By using probability of detection with size criteria as the comparison parameter, the superiorities of the proposed method against DTS, MSES, and HTS reached 53%, 52%, and 48%, respectively. It must be noted that the detection probabilities of DTS, MSES, and HTS in the second scenario were obtained in parallel with increasing their false detection probability up to 51%, 47%, and 48% while false detection probability for the proposed method in this scenario was 5% which doesn't show the meaningful increase due to its value in the first scenario.

5. Conclusion

In this manuscript, a new method is introduced for separating sperms from other semen particles in microscopic videos. In the proposed method, firstly a hypothesis testing function is defined to determine the dependence of each pixel to sperm or other particles. Then, each hypothesis is evaluated using a decision function which is constructed by mapping the wavelet sub-bands of each video frame to several bit-planes. In order to evaluate the performance of the proposed method, two scenarios are carried out based on microscopic videos of semen specimens containing different densities of sperms. The first scenario belonged to semen specimens with low densities of sperms and the second one dealt with specimens with high densities of sperms. In both scenarios, the performance of the proposed algorithm is compared with some existing methods (DTS, MSES, and HTS) by using three standard parameters. The first parameter is probability of detection when the detected sperm is defined as sperm with correct position in frame. The second parameter is probability of detection when the detected sperm is considered as a sperm and at least 90% of its pixels are detected correctly. The third parameter is probability of false detection. The results show the superiority of the proposed method in both of scenarios using all above mentioned parameters. In the first scenario, the proposed method detected 85% of sperms with size criteria which is at least 40% improvement compared with other existing methods. Also, using detection probability without size criteria, the proposed method shows at least 37% improvement compared with other existing methods. These improvements are obtained in false detection probability equal with 4% for the proposed method which shows no degradation compared with other methods. Although in the second scenario the detection parameters of all methods decreases due to high density of sperms, the superiority of the proposed method compared with other techniques increases in this scenario. In captured videos with high densities of sperms, the proposed algorithm shows at least 48% and 38% improvements

compared with other methods in detection probability with and without size criteria, respectively. Finally, in this scenario, the improvement in detection using the proposed method is paralleled with improvement in false detection parameter in such a way that the false detection probability of the proposed method is at least 42% better than other techniques. Consequently, it can be concluded that the proposed method may be used as a suitable alternative for detecting sperms in microscopic videos especially in semen specimens with high densities of sperms.

Acknowledgements

The authors are thankful to Dr Shahrokh Farahmand for faithful discussions and editing parts of this article.

References

1. Speroff L, Fritz MA. Clinical gynecologic endocrinology and infertility: Lippincott Williams & Wilkins; 2004.
2. Regulated Fertility Services: A commissioning aid, Department of Health, UK, June 2009. Available at: http://dh.gov.uk/prod_consum_dh/groups/dh_digitalassets/documents/digitalasset/dh_101068.pdf. Accessed Jan 28, 2013.
3. Wenzhong Y, Shuqun S. Automatic Chromosome Counting Algorithm Based on Mathematical Morphology. Journal of Data Acquisition & Processing. 2008;23(9):1004-9037.
4. Menkveld R, Wong WY, Lombard CJ, Wetzels AM, Thomas CM, Merkus HM, et al. Semen parameters, including WHO and strict criteria morphology, in a fertile and subfertile population: an effort towards standardization of in-vivo thresholds. Hum Reprod. 2001 Jun;16(6):1165-71.
5. Leung C, Lu Z, Esfandiari N, Casper RF, Sun Y, editors. Detection and tracking of low contrast human sperm tail. Automation Science and Engineering (CASE), 2010 IEEE Conference on; 2010: IEEE.
6. Shi LZ, Nascimento J, Chandsawangbhuwana C, Berns MW, Botvinick EL. Real-time automated tracking and trapping system for sperm. Microsc Res Tech. 2006 Nov;69(11):894-902.
7. Abbiramy V, Shanthi V, Allidurai C, editors. Spermatozoa detection, counting and tracking in video streams to detect asthenozoospermia. Signal and Image Processing (ICSIP), 2010 International Conference on; 2010: IEEE.
8. Abbiramy V, Shanthi V. Spermatozoa segmentation and morphological parameter analysis based detection of teratozoospermia. International Journal of Computer Applications IJCA. 2010;3(7):19-23.
9. Carrillo H, Villarreal J, Sotaquira M, Goelkel M, Gutierrez R, editors. A computer aided tool for the assessment of human sperm morphology. Bioinformatics and Bioengineering, 2007 BIBE 2007 Proceedings of the 7th IEEE International Conference on; 2007: IEEE.
10. Carrillo H, Villarreal J, Sotaquira M, Goelkel A, Gutierrez R, editors. Spermatozoon segmentation towards an objective analysis of human sperm morphology. Image and Signal Processing and Analysis, 2007 ISPA 2007 5th International Symposium on; 2007: IEEE.
11. Acosta AA, Kruger TF.Menkveld R, Kruger T. Evaluation of sperm morphology by light microscopy. Human Spermatozoa in Assisted Reproduction. 1996:89-107.
12. Mazzilli F, Rossi T, Delfino M, Nofroni I. Application of the upgraded image superimposition system (SIAS) to the assessment of sperm kinematics. Andrologia. 1999 Jul;31(4):187-94.
13. Wu Q, Merchant F, Castleman KR. Microscope image processing: Academic press; 2008.
14. Xuan ZL, Yan WZ, editors. The sperm video segmentation based on dynamic threshold. Machine Learning and Cybernetics (ICMLC), 2010 International Conference on; 2010: IEEE.
15. Cui C. Per-Pixel Background Estimation In Video Microscopy Using Frame Grouping and Wavelet Based Image Fusion. 2009.
16. Liu JC, Hwang WL, Chen MS, Tsai JW, Lin CH, editors. Wavelet based active contour model for object tracking. Image Processing, 2001 Proceedings 2001 International Conference on; 2001: IEEE.
17. Yi W, Park K, Paick J, editors. Parameterized characterization of elliptic sperm heads using Fourier representation and wavelet transform. Engineering in Medicine and Biology Society, 1998 Proceedings of the 20th Annual International Conference of the IEEE; 1998: IEEE.
18. Meijering E, Smal I, Dzyubachyk O, Olivo-Marin JC. Time-lapse imaging. Microscope Image Processing. 2008:401-40.

19. Zimmer C, Labruyere E, Meas-Yedid V, Guillen N, Olivo-Marin JC. Segmentation and tracking of migrating cells in videomicroscopy with parametric active contours: A tool for cell-based drug testing. Medical Imaging, IEEE Transactions on. 2002;21(10):1212-21.
20. Wählby C, SINTORN IM, Erlandsson F, Borgefors G, Bengtsson E. Combining intensity, edge and shape information for 2D and 3D segmentation of cell nuclei in tissue sections. Journal of Microscopy. 2004;215(1):67-76.
21. Yang X, Li H, Zhou X. Nuclei segmentation using marker-controlled watershed, tracking using mean-shift, and kalman filter in time-lapse microscopy. Circuits and Systems I: Regular Papers, IEEE Transactions on. 2006;53(11):2405-14.
22. Mallat S. A wavelet tour of signal processing. 1998. Academic, San Diego, CA.
23. Gonzalez RC, Woods RE. Digital Image Processing: Pearson/Prentice Hall; 2008.
24. Haralick RM, Shapiro LG. Computer and Robot Vision. Addison-Wesley Pub. Co. Boston,1992.
25. Liu B, Chen X, Ma C, Zhang D, Zhou X, He Y, editors. Research on threshold segmentation in tracking technology of moving objects. Industrial Mechatronics and Automation (ICIMA), 2010 2nd International Conference on; 2010: IEEE.
26. Bai W, Liu J, Chen G, editors. Segmentation of white rat sperm image. Proceedings of SPIE, the International Society for Optical Engineering; 2011: Society of Photo-Optical Instrumentation Engineers.
27. Mortimer ST. A critical review of the physiological importance and analysis of sperm movement in mammals. Human Reproduction Update. 1997;3(5):403-39.